

# Monte Carlo Calculations of Nuclei

Steven C. Pieper

Physics Division, Argonne National Laboratory,  
Argonne, IL 60439, USA

**Abstract.** Nuclear many-body calculations have the complication of strong spin- and isospin-dependent potentials. In these lectures I discuss the variational and Green's function Monte Carlo techniques that have been developed to address this complication, and present a few results.

## 1 Introduction

A major goal in nuclear physics is to understand how nuclear binding, stability, and structure arise from the underlying interactions between individual nucleons. To achieve this goal, we must both determine the Hamiltonian to be used, and devise reliable methods for many-body calculations with it. In principle quantum chromodynamics can prescribe the nuclear Hamiltonian, but it will be a long time before this will be done with useful accuracy. Thus the nuclear Hamiltonian is determined phenomenologically, and our knowledge of it is refined, in part, by the many-body calculations we make with it. A large amount of empirical information about the nucleon-nucleon scattering problem has been accumulated over time, resulting in ever more sophisticated  $NN$  potential models. These models have strong spin and isospin dependence, and spin and orbital angular momentum are mixed by a strong tensor interaction. In addition the three-nucleon interaction must be considered in realistic calculations, however there is very little experimental knowledge of it.

Thus the nuclear many-body Hamiltonian is significantly more complicated than those encountered most atomic and condensed-matter problems, and progress in accurate nuclear ground state calculations has been quite slow. As Table 1 shows, it took 30 years to progress from the two-body ground state to the three-body one; the four-body problem was solved in a few more years. It then took some time until ongoing advances in computational resources, particularly the advent of massively parallel computers, allowed us to apply sophisticated quantum Monte Carlo methods to the study of light  $p$ -shell nuclei, up to 8-body nuclei.

Quantum Monte Carlo methods for central interactions are discussed in R. Guardiola's contribution to this volume; here I will concentrate on the complications due to the state-dependence of the nuclear forces. The nuclear Hamiltonian is presented in the next section, variational Monte Carlo (VMC) for nuclei is presented in Sec. 3 and Green's function Monte Carlo (GFMC) in Sec. 4. Finally a very few recent results are given in the last section. The

RECEIVED  
NOV 04 1997  
OSTI

DISTRIBUTION OF THIS DOCUMENT IS UNLIMITED

MASTER

The submitted manuscript has been authored by a contractor of the U. S. Government under contract No. W-31-109-ENG-38. Accordingly, the U. S. Government retains a nonexclusive, royalty-free license to publish or reproduce the published form of this contribution, or allow others to do so, for U. S. Government purposes.

### **DISCLAIMER**

This report was prepared as an account of work sponsored by an agency of the United States Government. Neither the United States Government nor any agency thereof, nor any of their employees, makes any warranty, express or implied, or assumes any legal liability or responsibility for the accuracy, completeness, or usefulness of any information, apparatus, product, or process disclosed, or represents that its use would not infringe privately owned rights. Reference herein to any specific commercial product, process, or service by trade name, trademark, manufacturer, or otherwise does not necessarily constitute or imply its endorsement, recommendation, or favoring by the United States Government or any agency thereof. The views and opinions of authors expressed herein do not necessarily state or reflect those of the United States Government or any agency thereof.

# **DISCLAIMER**

**Portions of this document may be illegible  
in electronic image products. Images are  
produced from the best available original  
document.**

Table 1. Exact (1%) realistic ground-state solutions.

Nucleus	Method	First Done	Floating Ops.	Computer	Time
$^2\text{H}$	Variational, Coupled Dif Eq	1940's - 1953	$\sim 50 \times 10^3$	Illiac-I	15 min (+ 5 for printing)
$^3\text{H}$	34 Chn Faddeev	1984	$100 \times 10^9$	Cray XMP	30 min
$^4\text{He}$	GFMC	1987	$15 \times 10^{12}$	Cray 2	40 hr
$^5\text{He}$	GFMC	1993	$100 \times 10^{12}$	Cray C90	100 hr
$^6\text{Li}$	GFMC	1995	$1 \times 10^{13}$	IBM SP1	40 nodes, 150 hr
$^7\text{Li}$	GFMC	end 95	$1.5 \times 10^{15}$	IBM SP2	100 nodes, 50 hr
$^8\text{Be}$	GFMC	end 96	$7 \times 10^{15}$	IBM SP2	25 nodes, 120 hr

specific methods and results presented here are from the work of the Argonne, Los Alamos, and Urbana groups; a complete description of our VMC and GFMC calculations may be found in [1]. A good pedagogical discussion of the nuclear VMC method, including a complete, simplified, program may be found in [2].

## 2 The Nuclear Hamiltonian

In this section I discuss a slightly simplified version of the Hamiltonian used in our calculations. Specifically the complications of charge dependence and of the full electromagnetic potential will be only briefly mentioned. The complexity of the nuclear Hamiltonian is dictated by a number of experimental observations:

Nuclear forces are of short but finite range. The binding energy for few-body nuclei increases as the number of pairs, from 2.2 MeV in  $^2\text{H}$  to 2.8 MeV/pair in  $^3\text{H}$  to 4.7 MeV/pair in  $^4\text{He}$ . For larger nuclei the binding energy per nucleon is approximately constant at 8 MeV/A. This indicates that nuclear forces are short-range, roughly equal to the radius of  $^4\text{He}$ , or  $\sim 1.7$  fm.

As is indicated by the fact that the low-energy  $S$ -wave phase shifts are positive, the nuclear force is attractive at intermediate and long ranges. However, the nuclear force has a short-ranged repulsive core. The  $^1S_0$  phase shifts turn negative for  $E_{lab} \sim 250$  MeV, while the  $^1D_2$  phase shifts remain positive up to 800 MeV. This can be understood as a repulsive core of  $\sim 0.6$  fm, which is masked in the  $D$ -wave by the centrifugal barrier.

The force depends on the spins and isospins of the nucleons. Only the  $S = 1$ ,  $T = 0$  channel has a bound state, while the phase shifts are very different in different  $S$ ,  $T$  channels. In addition, the structure of the deuteron

indicates that there is a tensor force. The deuteron has a quadrupole moment, a magnetic moment that requires a D-state, and an asymptotic D/S state ratio. In scattering states there are finite mixing parameters  $\epsilon_J$  (transitions between  $L = J - 1$  and  $L = J + 1$  states). Finally, there is also a spin-orbit force; the energy-dependence of the  ${}^3P_{0,1,2}$  partial wave phase shifts requires both tensor and spin-orbit forces.

Our Hamiltonian includes a nonrelativistic one-body kinetic energy, the Argonne  $v_{18}$  two-nucleon potential [3] and the Urbana IX three-nucleon potential [4],

$$H = \sum_i K_i + \sum_{i < j} v_{ij} + \sum_{i < j < k} V_{ijk} . \quad (1)$$

Ignoring the difference in proton and neutron masses, the kinetic energy operator is

$$K_i = -\frac{\hbar^2}{2m} \nabla_i^2 . \quad (2)$$

The Argonne  $v_{18}$  potential can be written as a sum of electromagnetic and one-pion-exchange terms and a shorter-range phenomenological part,

$$v_{ij} = v_{ij}^\gamma + v_{ij}^\pi + v_{ij}^R . \quad (3)$$

The electromagnetic terms include one- and two-photon-exchange Coulomb interactions, vacuum polarization, Darwin-Foldy, and magnetic moment terms, with appropriate proton and neutron form factors.

Ignoring the difference between charged and neutral pion masses, the one-pion-exchange part of the potential can be written as

$$v_{ij}^\pi = f_\pi^2 \frac{1}{3} m_\pi c^2 X_{ij}^\pi \tau_i \cdot \tau_j , \quad (4)$$

$$X_{ij}^\pi = Y(r) \sigma_i \cdot \sigma_j + T(r) S_{ij} . \quad (5)$$

Here  $Y(r)$  and  $T(r)$  are the normal Yukawa and tensor functions with a cutoff specified by a parameter  $c$ :

$$Y(r) = \frac{1}{m_\pi r} e^{-m_\pi r} C(r) , \quad (6)$$

$$T(r) = \left[ 1 + \frac{3}{m_\pi r} + \frac{3}{(m_\pi r)^2} \right] \frac{1}{m_\pi r} e^{-m_\pi r} C^2(r) , \quad (7)$$

$$C(r) = 1 - e^{-cr^2} , \quad (8)$$

The  $\sigma_i$  are the  $2 \times 2$  Pauli spin matrices; the nucleon spin operator is  $S_i = \frac{1}{2} \sigma_i$ . The  $\tau_i$  are the same Pauli matrices acting in isospin space; our convention is that  $\tau(z) = +1$  for protons and  $-1$  for neutrons. The tensor operator,  $S_{ij}$ , is introduced below.

The one-pion-exchange and the remaining phenomenological part of the potential can be written as a sum of eighteen operators, which is where the name  $v_{18}$  comes from:

$$v_{ij}^\pi + v_{ij}^R = \sum_{p=1,18} v_p(r_{ij}) O_{ij}^p . \quad (9)$$

The first fourteen are charge-independent,

$$O_{ij}^{p=1,14} = [1, (\sigma_i \cdot \sigma_j), S_{ij}, (\mathbf{L} \cdot \mathbf{S}), \mathbf{L}^2, \mathbf{L}^2(\sigma_i \cdot \sigma_j), (\mathbf{L} \cdot \mathbf{S})^2] \otimes [1, (\tau_i \cdot \tau_j)] \quad (10)$$

and the last four break charge independence. In addition to the one-pion  $Y(r)$  and  $T(r)$ , the  $v_p(r)$  contain intermediate- and short-range functions which are determined by fitting  $NN$  scattering data.

The potential was fit directly to the Nijmegen  $NN$  scattering data base [5, 6], which contains 1787  $pp$  and 2514  $np$  data in the range 0 – 350 MeV, with a  $\chi^2$  per datum of 1.09. It was also fit to the  $nn$  scattering length measured in  $d(\pi^-, \gamma)nn$  experiments and the deuteron binding energy.

A brief discussion of the effects of some of the operators in the potential follows. Nuclear isospin is (approximately) conserved by the strong interaction. This means that it is useful to project a pair of nucleons into states of good total isospin:

$$T = 0 \text{ pair : } \frac{1}{\sqrt{2}} [ |pn\rangle - |np\rangle ] ; \quad (11)$$

$$T = 1 \text{ pairs : } |pp\rangle, \frac{1}{\sqrt{2}} [ |pn\rangle + |np\rangle ], |nn\rangle . \quad (12)$$

These are eigenstates of  $\tau_i \cdot \tau_j$ :

$$\tau_i \cdot \tau_j |T = 0\rangle = -3 |T = 0\rangle ; \quad (13)$$

$$\tau_i \cdot \tau_j |T = 1\rangle = 1 |T = 1\rangle . \quad (14)$$

Thus operators with or without  $\tau \cdot \tau$  allow for different potentials in  $T = 0$ ,  $T = 1$  states. Similarly  $\sigma_i \cdot \sigma_j$  results in different forces in spin-singlet and spin-triplet states.

The tensor operator is

$$S_{12} = 3 \sigma_1 \cdot \hat{r}_{12} \sigma_2 \cdot \hat{r}_{12} - \sigma_1 \cdot \sigma_2 . \quad (15)$$

This produces a D-state in the  $S = 1$ ,  $J = 1$  deuteron:

$$|J = 1, M_J\rangle = \sqrt{1 - \beta^2} |^3S_1\rangle + \beta |^3D_1\rangle ; \quad \beta^2 \sim 6\% . \quad (16)$$

The spin-orbit operator is

$$\mathbf{L} \cdot \mathbf{S} = \left[ \frac{1}{2i} (\mathbf{r}_i - \mathbf{r}_j) \times (\nabla_i - \nabla_j) \right] \cdot \left[ \frac{1}{2} (\sigma_i + \sigma_j) \right] , \quad (17)$$

and gives different forces in  $^3P_0$ ,  $^3P_1$ , and  $^3P_2$  waves.  $\mathbf{L}^2$  and  $(\mathbf{L} \cdot \mathbf{S})^2$  operators are one (non-unique) way of fine-tuning the interaction in  $L = 2, 3$  (D,F) waves. Other potential models use  $\mathbf{P}^2$  terms instead of  $\mathbf{L}^2$ , but this can result in much more difficult many-body calculations.

The tensor-isospin potential is very important in nuclear physics both because it provides most of the binding and because it greatly complicates calculations. It arises from pion exchange which provides the longest-range strong interaction ( $v^\pi \sim e^{-r/m_\pi}$ ,  $m_\pi \sim 0.7 \text{ fm}^{-1}$ ), and dominates the nucleon-nucleon interaction. As an example, consider the binding of the deuteron:

$$E_{2H} = 2.224 \text{ MeV} , \\ = +(19.81 \text{ kinetic}) - (21.28 v^\pi) - (0.75 \text{ other } v_{ij}) . \quad (18)$$

Typically  $v^\pi$  provides 70% of  $v_{ij}$  in other nuclei. As shown above,  $v^\pi$  has  $\sigma_i \cdot \sigma_j$ ,  $\tau_i \cdot \tau_j$  and  $S_{ij}$ ,  $\tau_i \cdot \tau_j$  terms and it turns out that  $S_{ij}$  is typically 70% of  $v^\pi$ ; without the  $S_{ij}$ ,  $\tau_i \cdot \tau_j$  term, no nuclei would be bound! But,

$$\int d^2 \Omega_{r_{12}} S_{12} = \int d^2 \Omega_{r_{12}} S_{12} \sigma_i \cdot \sigma_j = 0 , \quad (19)$$

while

$$\int d^2 \Omega_{r_{12}} (S_{12})^2 = 24\pi . \quad (20)$$

So in  $E = \langle \Psi_{G.S.} | H | \Psi_{G.S.} \rangle$  we need a  $S_{ij}$  operator in  $\Psi_{G.S.}$  to get the  $v^\pi$  contribution. This results in the 6% D-state in the deuteron.

The Urbana series of three-nucleon potentials is written as a sum of two-pion-exchange and shorter-range phenomenological terms,

$$V_{ijk} = V_{ijk}^{2\pi} + V_{ijk}^R . \quad (21)$$

The two-pion-exchange term can be expressed simply as

$$V_{ijk}^{2\pi} = \sum_{cyclic} A_{2\pi} \{X_{ij}^\pi, X_{jk}^\pi\} \{\tau_i \cdot \tau_j, \tau_j \cdot \tau_k\} + C_{2\pi} [X_{ij}^\pi, X_{jk}^\pi] [\tau_i \cdot \tau_j, \tau_j \cdot \tau_k] , \quad (22)$$

where  $X_{ij}^\pi$  is defined in Eq. 5, For the Urbana models  $C_{2\pi} = \frac{1}{4} A_{2\pi}$ , as in the original Fujita-Miyazawa model [7]. The shorter-range phenomenological term is given by

$$V_{ijk}^R = \sum_{cyclic} U_0 T^2(r_{ij}) T^2(r_{jk}) . \quad (23)$$

The parameters for model IX are  $A_{2\pi} = -0.0293 \text{ MeV}$  and  $U_0 = 0.0048 \text{ MeV}$ . They have been determined by fitting the density of nuclear matter and the binding energy of  $^3\text{H}$  in conjunction with the Argonne  $v_{18}$  interaction. The  $V_{ijk}^R$  certainly should have other terms [8], however we need additional data to obtain their strengths; presumably a part of it is also really due to relativistic effects [9, 10, 11].

In light nuclei we find

$$\langle V^{NNN} \rangle \sim .04 \langle v^{NN} \rangle , \\ \sim .25 \langle H \rangle . \quad (24)$$

where the second line is due to the large cancelation of  $T$  and  $v$ . We expect a similar ratio for the four-body potential:

$$\begin{aligned} \langle v^{4N} \rangle &\sim .04 \langle V^{NNN} \rangle, \\ &\sim .01 \langle H \rangle. \end{aligned} \quad (25)$$

Calculations are just approaching this accuracy.

### 3 Variational Monte Carlo

The variational method can be used to obtain approximate solutions to the many-body Schrödinger equation,  $H\Psi = E\Psi$ , for a wide range of nuclear systems, including few-body nuclei, light closed shell nuclei, and nuclear and neutron matter [12]. A suitably parameterized wave function,  $\Psi_T$ , is used to calculate an upper bound to the exact ground-state energy,

$$E_T = \frac{\langle \Psi_T | H | \Psi_T \rangle}{\langle \Psi_T | \Psi_T \rangle} \geq E_0. \quad (26)$$

The parameters in  $\Psi_T$  are varied to minimize  $E_T$ , and the lowest value is taken as the approximate ground-state energy.

Upper bounds to excited states are also obtainable, either from standard VMC calculations if they have different quantum numbers from the ground state, or from small-basis diagonalizations if they have the same quantum numbers. The corresponding  $\Psi_T$  can then be used to calculate other properties, such as particle density or electromagnetic moments, or it can be used as the starting point for a Green's function Monte Carlo calculation.

#### 3.1 Wave Function

Here I discuss a simplified form of  $\Psi_T$ ; see [1] for the complete form used in current calculations,

$$|\Psi_T\rangle = \mathcal{S} \prod_{i < j}^A F_{ij} |\Phi\rangle; \quad (27)$$

The complete  $\Psi_T$  also includes three-body correlations induced by  $V_{ijk}$ .

The  $\Phi$  is the one-body part; it determines the  $J, M_J, T, T_z$  of the nucleus, and is completely antisymmetric. The  $F_{ij}$  are the two-body correlations induced by  $v_{ij}$ . Therefore,  $F_{ij}$  is written in terms of a subset of the operators in  $v_{ij}$ :

$$\begin{aligned} F_{ij} &= \sum_p f_p(r_{ij}) O_{ij}^{(p)} \\ &= f_c(r_{ij}) + f_\tau(r_{ij}) \tau_i \cdot \tau_j + \cdots f_{t\tau}(r_{ij}) S_{ij} \tau_i \cdot \tau_j + \cdots \end{aligned} \quad (28)$$

The  $f_p(r)$  are the solutions of Euler-Lagrange equations; see [2] for an introduction to these and [13] for details on the complete  $f_p(r)$  used in modern calculations.

These operators do not commute, for example

$$[\sigma_i \cdot \sigma_j, \sigma_i \cdot \sigma_k] = 2i(\sigma_i \times \sigma_j) \cdot \sigma_k. \quad (29)$$

Hence,  $[F_{ij}, F_{ik}] \neq 0$ , and we must use a symmetrized product. As an example, for  ${}^3\text{H}$ ,

$$\begin{aligned} \mathcal{S} \prod_{i < j} F_{ij} = \frac{1}{6} (F_{12}F_{13}F_{23} + F_{12}F_{23}F_{13} + F_{13}F_{12}F_{23} + F_{23}F_{13}F_{12} \\ + F_{13}F_{23}F_{12} + F_{23}F_{12}F_{13}). \end{aligned} \quad (30)$$

Note that it has  $[\frac{A(A-1)}{2}]!$  terms!

The  $\Psi_T$  must be translationally invariant. The  $F_{ij}$  are functions of  $r_i - r_j$  and hence satisfy this. If  $\Phi$  has dependence on  $r_i$ , then we use  $\tilde{r}_i$  in  $\Phi$ , where

$$\tilde{r}_i = r_i - R_{cm}; \quad R_{cm} = \frac{1}{A} \sum_i r_i. \quad (31)$$

The  $\Psi_T$  must also describe a localized (bound state) system. This is achieved by having

$$F_{ij}(r_{ij}) \rightarrow 0, \quad r_{ij} \rightarrow \infty, \quad (32)$$

or

$$\Phi(r_1, r_2, \dots, r_A) \rightarrow 0, \quad r_i \rightarrow \infty, \quad (33)$$

or some combination of these.

**Spin-isospin structure of  $\Psi_T$ .** Each nucleon can be a proton or neutron but total charge is conserved. Thus for  ${}^3\text{H}$  we can have  $pnn$ ,  $npn$ , or  $nnp$ . Each nucleon can be spin up or down and tensor correlations do not conserve the total spin ( $J = L + S$  is of course conserved); for  ${}^3\text{H}$  we can have  $\uparrow\uparrow\uparrow$ ,  $\uparrow\uparrow\downarrow$ ,  $\dots$ ,  $\downarrow\downarrow\downarrow$ . Thus  ${}^3\text{H}$  has  $3 \times 8 = 24$  components in its spin-isospin structure.

The number of components can be reduced by noting that  ${}^3\text{H}$  has total isospin  $T = \frac{1}{2}$ , so one really needs only two states:

$$|T = \frac{1}{2}, a\rangle = \frac{1}{\sqrt{2}}(|pnn\rangle - |npn\rangle), \quad (34)$$

and

$$|T = \frac{1}{2}, b\rangle = \frac{1}{\sqrt{3}}[\frac{1}{\sqrt{2}}(|pnn\rangle + |npn\rangle) - \sqrt{2}|nnp\rangle]. \quad (35)$$

The 3rd linearly independent state does not contribute:

$$|T = \frac{3}{2}\rangle = \frac{1}{\sqrt{3}}(|pnn\rangle + |npn\rangle + |nnp\rangle). \quad (36)$$

The number of components in  $\Psi_T$  grows rapidly with the number of nucleons, as is shown in Table 2. Calculations of the sort being described here

Table 2. Number of spin-isospin components

$A$	$Z$	$T$	$N_{spin}^a$	$N_{charge}^b$	$N_{isospin}^c$	$N_{total}^d$
3	1	1/2	8	3	2	16
4	2	0	16	6	2	32
6	2	1	64	15	9	576
6	3	0	64	20	5	320
7	2	3/2	128	21	14	1792
7	3	1/2	128	35	14	1792
8	2	2	256	28	20	5120
8	3	1	256	56	28	7168
8	4	0	256	70	14	3584
12	6	0	4096	924	132	540,672
16	8	0	65,536	12,870	1430	93,716,480
40	20	0	1.0995E12	1.3785E11	6.5641E9	7.2173E21

<sup>a</sup>  $2^A$ <sup>b</sup>  $\binom{A}{2}$ <sup>c</sup>  $\frac{2T+1}{A/2+T+1} \binom{A}{A/2+T}$ <sup>d</sup>  $N_{spin} \times N_{isospin}$ 

are currently feasible up to only  $A = 8$ . Cluster methods have been used for VMC calculations of larger nuclei [14], and these are being developed for the GFMC.

For  ${}^3H$  and  ${}^4He$ ,  $\Phi$  contains just the spin and isospin structure and has no spatial dependence:

$$\begin{aligned}
 |\Phi({}^3H, M_J = \tfrac{1}{2})\rangle = & \frac{1}{\sqrt{6}} ( |p\uparrow n\uparrow n\downarrow\rangle - |p\uparrow n\downarrow n\uparrow\rangle \\
 & + |n\downarrow p\uparrow n\uparrow\rangle - |n\uparrow p\uparrow n\downarrow\rangle \\
 & + |n\uparrow n\downarrow p\uparrow\rangle - |n\downarrow n\uparrow p\uparrow\rangle ) . \quad (37)
 \end{aligned}$$

Thus the 24-component  $\Phi$  has 6 elements  $= \pm \frac{1}{\sqrt{6}}$ ; the rest are 0. It is totally antisymmetric and has total isospin and angular momentum  $T = 1/2$ ,  $J = 1/2$ . For  ${}^4He$  we have

$$\begin{aligned}
 |\Phi({}^4He)\rangle = & \frac{1}{\sqrt{24}} ( |p\uparrow p\downarrow n\uparrow n\downarrow\rangle - |p\downarrow p\uparrow n\uparrow n\downarrow\rangle \\
 & + |p\downarrow p\uparrow n\downarrow n\uparrow\rangle - |p\uparrow p\downarrow n\downarrow n\uparrow\rangle \\
 & - |p\uparrow n\uparrow p\downarrow n\downarrow\rangle + \dots ) . \quad (38)
 \end{aligned}$$

It has 24 non-zero terms in a 96-component vector. An antisymmetric state of more than four nucleons cannot be made in just spin and isospin; one needs spatial degrees of freedom (the p-shell).

**Operators in  $\Psi_T$ .** The full  $|\Psi_T\rangle$  is a sum of terms like

$$F_{nm} \cdots F_{23} F_{13} F_{12} |\Phi\rangle \quad (39)$$

where all orderings of the  $F_{ij}$  are used. Each  $F_{ij}$  is a (very) sparse matrix operating on a column vector in spin-isospin space to produce a resultant vector.

For example, consider the  $\sigma_i \cdot \sigma_j$  operator

$$\sigma_i \cdot \sigma_j = 2(\sigma_i^+ \sigma_j^- + \sigma_i^- \sigma_j^+) = 2P_{ij}^\sigma - 1 \quad (40)$$

where  $P_{ij}^\sigma$  exchanges the spin of  $i$  and  $j$ . For  ${}^3H$  and considering just the spin of the nucleons:

$$\Psi = \begin{pmatrix} a_{\uparrow\uparrow\uparrow} \\ a_{\uparrow\uparrow\downarrow} \\ a_{\uparrow\downarrow\uparrow} \\ a_{\uparrow\downarrow\downarrow} \\ a_{\downarrow\uparrow\uparrow} \\ a_{\downarrow\uparrow\downarrow} \\ a_{\downarrow\downarrow\uparrow} \\ a_{\downarrow\downarrow\downarrow} \end{pmatrix}; \quad \sigma_2 \cdot \sigma_3 \Psi = \begin{pmatrix} a_{\uparrow\uparrow\uparrow} \\ 2a_{\uparrow\downarrow\uparrow} - a_{\uparrow\uparrow\downarrow} \\ 2a_{\uparrow\uparrow\downarrow} - a_{\uparrow\downarrow\uparrow} \\ a_{\uparrow\downarrow\downarrow} \\ a_{\downarrow\uparrow\uparrow} \\ 2a_{\downarrow\downarrow\uparrow} - a_{\downarrow\uparrow\downarrow} \\ 2a_{\downarrow\uparrow\downarrow} - a_{\downarrow\downarrow\uparrow} \\ a_{\downarrow\downarrow\downarrow} \end{pmatrix}. \quad (41)$$

Note that  $\sigma_1$  is a "spectator" and that  $\sigma_i \cdot \sigma_j$  will not mix different isospin components. In 2-nucleon spin space this is the  $4 \times 4$  matrix

$$\sigma_i \cdot \sigma_j = \begin{pmatrix} 1 & 0 & 0 & 0 \\ 0 & -1 & 2 & 0 \\ 0 & 2 & -1 & 0 \\ 0 & 0 & 0 & 1 \end{pmatrix} \text{ acting on } \begin{pmatrix} a_{\uparrow\uparrow} \\ a_{\uparrow\downarrow} \\ a_{\downarrow\uparrow} \\ a_{\downarrow\downarrow} \end{pmatrix}. \quad (42)$$

Similarly, the tensor operator (Eq. 15) is

$$S_{ij} = 3 \begin{pmatrix} z^2 - 1/3 & z(x - iy) & z(x - iy) & (x - iy)^2 \\ z(x + iy) & -z^2 - 1/3 & x^2 + y^2 - 2/3 & -z(x - iy) \\ z(x - iy) & x^2 + y^2 - 2/3 & -z^2 + 1/3 & -z(x + iy) \\ (x + iy)^2 & -z(x + iy) & -z(x + iy) & z^2 - 1/3 \end{pmatrix}. \quad (43)$$

This is dense in the space of two nucleons but in an  $A$ -body nucleus, there will be  $A - 2$  spectators whose spins remain unchanged. Thus the  $A$ -body operator will be sparse with many  $4 \times 4$  blocks. Efficient programs for these calculations contain explicit code for the operators and do not use general sparse-matrix routines.

**Considerations for  $A > 4$ .** For nuclei with  $A > 4$ , the one-body part must have spatial dependence in order to be completely antisymmetric. As an example, for  ${}^6\text{Li}$ , the one-body part has the general form

$$|\Phi\rangle = \mathcal{A} \sum_{LS} \beta_{LS} |\Phi_6(LSJM T T_3)_{1234:56}\rangle. \quad (44)$$

The  $LS$  components of the single-particle wave function are given by

$$\begin{aligned} |\Phi_6(LSJM T T_3)_{1234:56}\rangle &= |\Phi_4(0000)_{1234}\phi_p^{LS}(R_{\alpha 5})\phi_p^{LS}(R_{\alpha 6}) \\ &\left\{ [Y_{1m_1}(\Omega_{\alpha 5})Y_{1m'_1}(\Omega_{\alpha 6})]_{LM_L} \times [\chi_5(\tfrac{1}{2}m_s)\chi_6(\tfrac{1}{2}m'_s)]_{SM_S} \right\}_{JM} \\ &\times [\nu_5(\tfrac{1}{2}t_3)\nu_6(\tfrac{1}{2}t'_3)]_{TT_3}. \end{aligned} \quad (45)$$

The  $\phi_p^{LS}(R_{\alpha k})$  are  $p$ -wave solutions of a particle of reduced mass  $\frac{4}{5}m_N$  in an effective  $\alpha$ - $N$  potential. They are functions of the distance between the center of mass of the  $\alpha$  core (which contains particles 1-4 in this partition) and nucleon  $k$ , and may be different for different  $LS$  components. The parameters of the effective  $\alpha$ - $N$  potential are variational parameters and do not necessarily represent a phenomenological  $\alpha$ - $N$  interaction. The antisymmetry operator  $\mathcal{A}$  sums, with appropriate minus signs, over all partitions of 6 nucleons into 4+2 subdivisions.

After other parameters in the trial function have been optimized, we make a series of calculations in which the  $\beta_{LS}$  may be different in the left- and right-hand-side wave functions to obtain the diagonal and off-diagonal matrix elements of the Hamiltonian and the corresponding normalizations and overlaps. We diagonalize the resulting energy matrices to find the  $\beta_{LS}$  eigenvectors. The one-body wave functions,  $\Phi$  are orthonormal, but the correlated  $\Psi_T$  are not. Hence the diagonalizations use generalized eigenvalue routines including overlap matrices.

### 3.2 The VMC Method

The energy expectation value of Eq.(26) is evaluated using Monte Carlo integration. A detailed technical description of the methods used here can be found in Refs. [13, 2, 15]. Monte Carlo sampling is done both in configuration space and in the order of operators in the symmetrized product of Eq.(27) by following a Metropolis random walk. The expectation value for an operator  $O$  is given by

$$\langle O \rangle = \frac{\sum_{p,q} \int d\mathbf{R} \Psi_p^\dagger(\mathbf{R}) O \Psi_q(\mathbf{R})}{\sum_{p,q} \int d\mathbf{R} \Psi_p^\dagger(\mathbf{R}) \Psi_q(\mathbf{R})}. \quad (46)$$

The subscripts  $p$  and  $q$  specify the order of operators in the left and right hand side wave functions, while the integration runs over the particle coordinates  $\mathbf{R} = (\mathbf{r}_1, \mathbf{r}_2, \dots, \mathbf{r}_A)$ . This multidimensional integration is facilitated by introducing a probability distribution,  $W_{pq}(\mathbf{R})$ , such that

$$\langle O \rangle = \frac{\sum_{p,q} \int d\mathbf{R} [\Psi_p^\dagger(\mathbf{R}) O \Psi_q(\mathbf{R}) / W_{pq}(\mathbf{R})] W_{pq}(\mathbf{R})}{\sum_{p,q} \int d\mathbf{R} [\Psi_p^\dagger(\mathbf{R}) \Psi_q(\mathbf{R}) / W_{pq}(\mathbf{R})] W_{pq}(\mathbf{R})}. \quad (47)$$

This probability distribution is taken to be

$$W_{pq}(\mathbf{R}) = |\text{Re}(\langle \Psi_{T,p}^\dagger(\mathbf{R}) \Psi_{T,q}(\mathbf{R}) \rangle)|, \quad (48)$$

which is constructed from the wave function,  $\Psi_T$ , but with only one operator order of the symmetrized product.

Expectation values of the kinetic energy and spin-orbit potential require the computation of first derivatives and diagonal second derivatives of the wave function. These are obtained by evaluating the wave function at  $6A$  slightly shifted positions of the coordinates  $\mathbf{R}$  and taking finite differences, as discussed in Ref. [13]. Potential terms quadratic in  $\mathbf{L}$  require mixed second derivatives, which can be obtained by additional wave function evaluations and finite differences. A rotation trick can be used to reduce the number of additional locations at which the wave function must be evaluated [16].

The heart of the VMC calculation is the Metropolis algorithm, an inherently serial algorithm which must be adapted to modern parallel computers. Since the bulk of the work in our variational calculations lies in the energy expectation value, the straightforward division of labor is to have one master processor perform the Metropolis walk while several slave processors calculate the energy and other expectation values for the configurations that the master generates. The number of slave processors that can be efficiently used is the ratio of the CPU time needed for expectation values to that needed to walk from one configuration to the next. We find that typically 50 processors can be used efficiently in a  ${}^7\text{Li}$  VMC calculation.

## 4 Green's Function (Diffusion) Monte Carlo

GFMC projects out the lowest energy ground state using

$$\Psi_0 = \lim_{\tau \rightarrow \infty} \exp[-(H - E_0)\tau] \Psi_T. \quad (49)$$

The eigenvalue  $E_0$  is calculated exactly while other expectation values are generally calculated neglecting terms of order  $|\Psi_0 - \Psi_T|^2$  and higher. In contrast, the error in the variational energy,  $E_T$ , is of order  $|\Psi_0 - \Psi_T|^2$ , and other expectation values calculated with  $\Psi_T$  have errors of order  $|\Psi_0 - \Psi_T|$ . GFMC for scalar potentials is presented in R. Guardiola's and J. Boronat's contributions to this volume; here I will discuss some of the complications due to the

state-dependence of the nuclear Hamiltonian. It is not possible to present all of the details necessary for a successful nuclear GFMC calculation; a rather complete discussion may be found in [1].

We use the  $\Psi_T$  of Eq.(27) as our initial trial function and define the propagated wave function  $\Psi(\tau)$  as

$$\Psi(\tau) = e^{-(H-E_0)\tau} \Psi_T; \quad (50)$$

obviously  $\Psi(\tau = 0) = \Psi_T$  and  $\Psi(\tau \rightarrow \infty) = \Psi_0$ . Introducing a small time step,  $\Delta\tau$ ,  $\tau = n\Delta\tau$ , gives

$$\Psi(\tau) = \left[ e^{-(H-E_0)\Delta\tau} \right]^n \Psi_T = G^n \Psi_T. \quad (51)$$

where  $G$  is the short-time Green's function. The  $\Psi(\tau)$  is represented by a vector function of  $\mathbf{R}$ , and the Green's function,  $G_{\alpha\beta}(\mathbf{R}', \mathbf{R})$  is a matrix function of  $\mathbf{R}'$  and  $\mathbf{R}$  in spin-isospin space, defined as

$$G_{\alpha\beta}(\mathbf{R}', \mathbf{R}) = \langle \mathbf{R}', \alpha | e^{-(H-E_0)\Delta\tau} | \mathbf{R}, \beta \rangle. \quad (52)$$

It is calculated with leading errors of order  $(\Delta\tau)^3$  as discussed below. Omitting spin-isospin indices for brevity,  $\Psi(\mathbf{R}_n, \tau)$  is given by

$$\Psi(\mathbf{R}_n, \tau) = \int G(\mathbf{R}_n, \mathbf{R}_{n-1}) \cdots G(\mathbf{R}_1, \mathbf{R}_0) \Psi_T(\mathbf{R}_0) d\mathbf{R}_{n-1} \cdots d\mathbf{R}_1. \quad (53)$$

#### 4.1 The Short-Time Propagator

The short-time propagator should allow as large a time step  $\Delta\tau$  as possible, since the total computational time for propagation is proportional to  $1/\Delta\tau$ . The first nuclear GFMC calculations [4, 17, 18] used the propagator obtained from the Feynman formulae. Ignoring three-nucleon interaction terms in  $H$ , it is given by

$$e^{-H\Delta\tau} = \left[ S \prod_{i<j} e^{-v_{ij}\Delta\tau/2} \right] e^{-K\Delta\tau} \left[ S \prod_{i<j} e^{-v_{ij}\Delta\tau/2} \right] + \mathcal{O}(\Delta\tau^3). \quad (54)$$

Note that it is useful to symmetrize the product of  $e^{-v_{ij}\Delta\tau/2}$  when  $[v_{ij}, v_{jk}] \neq 0$ , in order to reduce the error per iteration. The nuclear  $v_{ij}$  has a repulsive core of order GeV. The main error in the above propagator comes from terms in  $e^{-H\Delta\tau}$  having multiple  $v_{ij}$ , like  $v_{ij}Kv_{ij}(\Delta\tau)^3$  for example, which can become large when particles  $i$  and  $j$  are very close. In order to make them negligible, a rather small  $\Delta\tau \sim 0.1 \text{ GeV}^{-1}$  is used with the above propagator.

The matrix elements of the propagator are given by:

$$G_{\alpha\beta}(\mathbf{R}', \mathbf{R}) = \langle \alpha | \left[ \mathcal{S} \prod_{i < j} e^{-v_{ij}(\mathbf{r}'_{ij}) \Delta\tau/2} \right] \times G_0(\mathbf{R}', \mathbf{R}) \left[ \mathcal{S} \prod_{i < j} e^{-v_{ij}(\mathbf{r}_{ij}) \Delta\tau/2} \right] | \beta \rangle , \quad (55)$$

$$G_o(\mathbf{R}', \mathbf{R}) = \langle \mathbf{R}' | e^{-K\Delta\tau} | \mathbf{R} \rangle = \left[ \sqrt{\frac{m}{2\pi\hbar^2\Delta\tau}} \right]^{3A} \exp \left[ \frac{-(\mathbf{R}' - \mathbf{R})^2}{2\hbar^2\Delta\tau/m} \right] . \quad (56)$$

Remember that  $v_{ij}$  is an operator in spin-isospin space, so evaluating  $e^{-\frac{\Delta\tau}{2}v_{ij}}$  is nontrivial. Consider the first 6 operators:

$$O_{1-6} = 1, \tau \cdot \tau, \sigma \cdot \sigma, \sigma \cdot \sigma \tau \cdot \tau, S_{12}, S_{12} \tau \cdot \tau . \quad (57)$$

These form a closed algebra:

$$O_i O_j = \prod_{k=1}^6 K^{ijk} O_k , \quad (58)$$

where the  $K^{ijk}$  are just numbers. For example

$$\begin{aligned} (\sigma_1 \cdot \sigma_2)^2 &= (2P_\sigma - 1)^2 = 4P_\sigma^2 - 4P_\sigma + 1 = 5 - 4P_\sigma \\ &= 5 - 4\frac{1}{2}(\sigma_1 \cdot \sigma_2 - 1) = 3 - 2\sigma_1 \cdot \sigma_2 . \end{aligned} \quad (59)$$

Tables of  $K^{ijk}$  may be found in [19]. Thus

$$\begin{aligned} e^{-a\sigma_i \cdot \sigma_j} &= 1 - a\sigma_i \cdot \sigma_j + \frac{1}{2}a^2(\sigma_i \cdot \sigma_j)^2 - \dots , \\ &= 1 + \frac{3}{2}a^2 - \dots - (a - a^2 + \dots)\sigma_i \cdot \sigma_j , \\ &= \frac{1}{4}(3e^{-a} + e^{3a}) + \frac{1}{4}(e^{-a} - e^{3a})\sigma_i \cdot \sigma_j , \end{aligned} \quad (60)$$

where the last line may be verified by expanding the  $e^{-a}$  and  $e^{3a}$ . More complete formulas, including those for exponentiating  $S_{ij}$ , may be found in [15].

Evaluating  $L \cdot S$  involves gradients, so a first-order expansion is used when using the propagator of Eq. 54:

$$e^{-\frac{\Delta\tau}{2}v_{LS}(L \cdot S)_{ij}} \simeq \left[ 1 - \frac{\Delta\tau}{2}v_{LS}(L \cdot S)_{ij} \right] , \quad (61)$$

$$\begin{aligned} (L \cdot S)g_0(\mathbf{r}', \mathbf{r}) &= \frac{1}{i} \mathbf{r} \times \nabla \cdot (\sigma_i + \sigma_j) e^{-\frac{m}{2\hbar^2\Delta\tau}(\mathbf{r}' - \mathbf{r})^2} \\ &= \frac{1}{4i} \frac{m}{\hbar^2\Delta\tau} (\mathbf{r} \times \mathbf{r}') \cdot (\sigma_i + \sigma_j) g_0 . \end{aligned} \quad (62)$$

Note that

$$\mathbf{r} \times \mathbf{r}' = \mathbf{r} \times (\mathbf{r} + \Delta\mathbf{r}) = \mathbf{r} \times \Delta\mathbf{r} \sim \sqrt{\Delta\tau}, \quad (63)$$

since  $\Delta\mathbf{r}$  will be sampled from the free Green's function. Thus even though the explicit  $\Delta\tau$  cancel in Eqn. 61 and 62, the contribution of  $v_{LS}$  still, on the average, decreases as  $\Delta\tau$  decreases.

It is well known from studies of liquid helium [20] that including the exact two-body propagator allows much larger time steps. This short-time propagator is

$$G_{\alpha\beta}(\mathbf{R}', \mathbf{R}) = G_0(\mathbf{R}', \mathbf{R}) \langle \alpha | \left[ \mathcal{S} \prod_{i < j} \frac{g_{ij}(\mathbf{r}'_{ij}, \mathbf{r}_{ij})}{g_{0,ij}(\mathbf{r}'_{ij}, \mathbf{r}_{ij})} \right] | \beta \rangle, \quad (64)$$

where  $g_{ij}$  is the exact two-body propagator,

$$g_{ij}(\mathbf{r}'_{ij}, \mathbf{r}_{ij}) = \langle \mathbf{r}'_{ij} | e^{-H_{ij}\Delta\tau} | \mathbf{r}_{ij} \rangle, \quad (65)$$

$$H_{ij} = -\frac{\hbar^2}{m} \nabla_{ij}^2 + v_{ij}, \quad (66)$$

and  $g_{0,ij}$  is the free two-body propagator,

$$g_{0,ij}(\mathbf{r}'_{ij}, \mathbf{r}_{ij}) = \left[ \sqrt{\frac{\mu}{2\pi\hbar^2\Delta\tau}} \right]^3 \exp \left[ -\frac{(\mathbf{r}'_{ij} - \mathbf{r}_{ij})^2}{2\hbar^2\Delta\tau/\mu} \right], \quad (67)$$

where  $\mu = m/2$  is the reduced mass. All terms containing any number of the same  $v_{ij}$  and  $K$  are treated exactly in this propagator, as we have included the imaginary-time equivalent of the full two-body scattering amplitude. Eq. 64 still has errors of order  $(\Delta\tau)^3$ , however they are from commutators of terms like  $v_{ij}T v_{ik}(\Delta\tau)^3$  which become large only when both pairs  $ij$  and  $ik$  are close. Since this is a rare occurrence, the  $\Delta\tau$  of Eq. 65 can be five or more times larger than that used with Eq. 54.

To calculate  $g_{ij}$ , we use the techniques developed by Schmidt and Lee[21] for scalar interactions. The basic idea is to use the convolution equation to write  $g_{ij}$  as a product over  $N$  steps:

$$g_{ij}(\mathbf{r}_N, \mathbf{r}_0; \Delta\tau) = \prod_{i=1}^N g_{ij}(\mathbf{r}_i, \mathbf{r}_{i-1}; \epsilon), \quad (68)$$

with  $\epsilon = \Delta\tau/N$  and an implied integration over intermediate points. The very-short-time propagator,  $g_{ij}(\mathbf{r}_i, \mathbf{r}_{i-1}; \epsilon)$ , is evaluated using the methods of Eqn. 55-62 applied to one pair. The errors for  $g_{ij}(\Delta\tau)$  contain only even powers of  $1/N$ , starting with  $1/N^2$ . [21] By evaluating  $g_{ij}(\mathbf{r}, \mathbf{r}'; \Delta\tau)$  for several values of  $N$  (and consequently  $\epsilon$ ) and extrapolating to  $\epsilon \rightarrow 0$  the  $g_{ij}$  can be calculated with high ( $\sim 10$  digit) accuracy.

Calculating this propagator is computationally intensive. Therefore, prior to the GFMC calculation, we compute and store the the propagator on a grid. For a spin-independent interaction, the propagator  $g_{ij}$  would depend only upon the two magnitudes  $r'$  and  $r$  and the angle  $\cos(\theta) = \hat{r}' \cdot \hat{r}$  between them. Here, though, there is also a dependence upon the spin quantization axis. Rotational symmetry allows one to calculate the spin-isospin components of  $g_{ij}(\mathbf{r}', \mathbf{r})$  for any  $\mathbf{r}'$  and  $\mathbf{r}$  by simple SU3 spin rotations and values of  $g_{ij}$  on a grid of initial points  $\mathbf{r} = (0, 0, z)$  and final points  $\mathbf{r}' = (x', 0, z')$ . In addition, the fact that the propagator is Hermitian allows us to store only the values for  $z > z'$ .

Finally, including the three-body forces and the  $E_0$  in Eq.(52), the complete propagator is given by

$$G_{\alpha\beta}(\mathbf{R}', \mathbf{R}) = e^{E_0 \Delta\tau} G_0(\mathbf{R}', \mathbf{R}) \exp[-\sum (V_{ijk}^R(\mathbf{R}') + V_{ijk}^R(\mathbf{R})) \frac{\Delta\tau}{2}]$$

$$\langle \alpha | I_3(\mathbf{R}') | \gamma \rangle \langle \gamma | \left[ S \prod_{i < j} \frac{g_{ij}(\mathbf{r}'_{ij}, \mathbf{r}_{ij})}{g_{0,ij}(\mathbf{r}'_{ij}, \mathbf{r}_{ij})} \right] | \delta \rangle \langle \delta | I_3(\mathbf{R}) | \beta \rangle, \quad (69)$$

$$I_3(\mathbf{R}) = \left[ 1 - \frac{\Delta\tau}{2} \sum V_{ijk}^{2\pi}(\mathbf{R}) \right]. \quad (70)$$

The exponential of  $V_{ijk}^{2\pi}$  is expanded to first order in  $\Delta\tau$  thus, there are additional error terms of the form  $V_{ijk}^{2\pi} V_{i'j'k'}^{2\pi} (\Delta\tau)^2$ . However, they have negligible effect since  $V_{ijk}^{2\pi}$  has a magnitude of only a few MeV. It was verified that the results for  ${}^4\text{He}$  do not show any change, outside of statistical errors, when  $\Delta\tau$  is decreased from  $0.5 \text{ GeV}^{-1}$ .

The exact propagator of Eq. 65 can be computed for the full  $v_{18}$  potential, however the  $\mathbf{L}^2$  and  $(\mathbf{L} \cdot \mathbf{S})^2$  terms in the potential correspond to state-dependent changes of the mass appearing in the free Green's function. Since we do not know how to sample such a free Green's function, we cannot use the exact  $g_{ij}$  for the full potential, but rather must use one constructed for an approximately equivalent potential that does not contain quadratic  $\mathbf{L}$  terms. The difference between the desired and approximate potentials is computed perturbatively. For the rest of this paper, I ignore this complication and present results and equations as if the full potential is used in the GFMC propagator.

## 4.2 Mixed Estimates

The mixed expectation value of an operator  $O$  is defined as:

$$\langle O \rangle_{Mixed} = \frac{\langle \Psi_T | O | \Psi(\tau) \rangle}{\langle \Psi_T | \Psi(\tau) \rangle}$$

$$= \frac{\int d\mathbf{P}_n \Psi_T^\dagger(\mathbf{R}_n) OG(\mathbf{R}_n, \mathbf{R}_{n-1}) \cdots G(\mathbf{R}_1, \mathbf{R}_0) \Psi_T(\mathbf{R}_0)}{\int d\mathbf{P}_n \Psi_T^\dagger(\mathbf{R}_n) G(\mathbf{R}_n, \mathbf{R}_{n-1}) \cdots G(\mathbf{R}_1, \mathbf{R}_0) \Psi_T(\mathbf{R}_0)}, \quad (71)$$

where  $\mathbf{P}_n = \mathbf{R}_0, \mathbf{R}_1, \dots, \mathbf{R}_n$  denotes the ‘path’, and  $d\mathbf{P}_n = d\mathbf{R}_0 d\mathbf{R}_1 \cdots d\mathbf{R}_n$ . In GFMC, the integral over the paths is carried out stochastically. Generally, the required expectation values are calculated approximately from the variational  $\Psi_T$  and mixed expectation values. Let

$$\Psi(\tau) = \Psi_T + \delta\Psi(\tau). \quad (72)$$

Retaining only the terms of order  $\delta\Psi(\tau)$ , we obtain

$$\begin{aligned} \langle O(\tau) \rangle &= \frac{\langle \Psi(\tau) | O | \Psi(\tau) \rangle}{\langle \Psi(\tau) | \Psi(\tau) \rangle}, \\ &\approx \langle O(\tau) \rangle_{Mixed} + [\langle O(\tau) \rangle_{Mixed} - \langle O \rangle_T], \end{aligned} \quad (73)$$

where

$$\langle O \rangle_T = \frac{\langle \Psi_T | O | \Psi_T \rangle}{\langle \Psi_T | \Psi_T \rangle}. \quad (74)$$

More accurate evaluations of  $\langle O(\tau) \rangle$  are possible, [22] essentially by measuring the observable at the mid-point of the path. However, such estimates require a propagation twice as long as the mixed estimate.

An important exception to the above is the energy,  $E_0$  given by  $\langle H(\tau \rightarrow \infty) \rangle$ . The  $\langle H(\tau) \rangle_{Mixed}$  can be re-expressed as (Ref. [23])

$$\langle H(\tau) \rangle_{Mixed} = \frac{\langle \Psi_T | e^{-(H-E_0)\tau/2} H e^{-(H-E_0)\tau/2} | \Psi_T \rangle}{\langle \Psi_T | e^{-(H-E_0)\tau/2} e^{-(H-E_0)\tau/2} | \Psi_T \rangle}, \quad (75)$$

since the propagator  $\exp[-(H-E_0)\tau]$  commutes with the Hamiltonian. Thus  $\langle H(\tau) \rangle_{Mixed}$  approaches  $E_0$  in the limit  $\tau \rightarrow \infty$ , and furthermore, being an expectation value of  $H$ , it obeys the variational principle

$$\langle H(\tau) \rangle_{Mixed} \geq E_0. \quad (76)$$

Because the expectation values of the individual energy components, such as  $K$ ,  $v_{ij}$ , and  $V_{ijk}$ , are extrapolated by Eq. 73, while the total  $E_0$  is not, they may not sum to the correct total energy. Indeed, there must be a collective error in these individual terms equal to the total difference between the GFMC  $\langle H \rangle_{Mixed}$  and the VMC  $\langle H \rangle_T$ . This is illustrated in Table 3 for the case of  ${}^6\text{Li}$ , where the difference  $\langle H \rangle_{Mixed} - \langle H \rangle_T$  is  $-4.3$  MeV, and the sum of the individual  $\langle O \rangle$  is an additional  $-4.3$  MeV lower than  $\langle H \rangle$ . In this case, the individual corrections are comparable in magnitude to the collective error, but small compared to the total expectation values.

**Table 3.** Contributions to the GFMC  $\langle O(\tau) \rangle$  of Eq. 73 for  ${}^6\text{Li}$ . All quantities are in MeV.

	$\langle O \rangle_T$	$\langle O \rangle_{Mixed}$	$\langle O \rangle_{Mixed} - \langle O \rangle_T$	$\langle O \rangle$
$K$	143.8(4)	147.3(5)	3.5(7)	150.8(10)
$v_{ij}$	-165.6(4)	-172.4(5)	-6.8(7)	-179.3(10)
$V_{ijk}$	-5.2(1)	-6.2(1)	-1.0(1)	-7.2(1)
Sum	-27.0(1)	-31.3(1)	-4.3(1)	-35.6(1)
$H$	-27.0(1)	-31.3(1)	-	-31.3(1)

#### 4.3 Dependence of Results on $\tau$

For more than four nucleons, GFMC calculations suffer significantly from the well-known Fermion sign problem which is discussed elsewhere in this volume. The resulting exponential growth of the statistical errors as one propagates to larger  $\tau$  limits our calculations to  $\tau \leq 0.1 \text{ MeV}^{-1}$ , and for most cases we do not go beyond  $\tau = 0.06 \text{ MeV}^{-1}$ . This means that any errors in  $\Psi_T$  corresponding to excitations of less than  $\sim 10 \text{ MeV}$  will be damped out by less than  $1/e$ . If we write

$$\Psi_T = \Psi_0 + \sum_i \alpha_i \Psi_i, \quad (77)$$

where

$$H\Psi_i = (E_0 + E_i^*)\Psi_i, \quad (78)$$

then the GFMC  $E(\tau)$  will be

$$E(\tau) = E_0 + \frac{\sum_i \alpha_i^2 E_i^* \exp(-E_i^* \tau)}{1 + \sum_i \alpha_i^2 \exp(-E_i^* \tau)}, \quad (79)$$

and by fitting such a form to the computed  $E(\tau)$  one can hope to extract  $E_0$ .

Figure 1 shows such fits made for  ${}^4\text{He}$ , for which we could afford calculations with very small statistical errors. The solid curve is a fit with  $E_0 = -28.335 \text{ MeV}$ , excitation energies  $E_i^* = 20.2, 341, \text{ and } 1477 \text{ MeV}$ , and corresponding  $\alpha_i^2 = 0.0062, 0.0018, \text{ and } 0.00046$ . The lowest  $0^+$  excitation of  ${}^4\text{He}$  is at  $20.2 \text{ MeV}$  and this energy was not varied in the fit. The  $\chi^2$  of the fit is 19 for 31  $E(\tau)$  (25 degrees of freedom), so the  $E(\tau)$  are not statistically independent. The dashed curve shows a fit without the  $20.2 \text{ MeV}$  excitation; it gives  $\chi^2 = 23$  and  $E_0 = -28.28 \text{ MeV}$ . Finally, the heavy solid line with short dashed error bars shows the average of the  $E(\tau)$  for  $0.04 \leq \tau \leq 0.1$ :  $-28.300(15)$ . It appears that in this most favorable case, with high statistics, high first excited state, and large maximum  $\tau$ , we can see that including the first excited state improves the extrapolation marginally.

However, the extrapolated  $E_0$  is not significantly lower than a simple average of the  $E(\tau)$  for  $0.04 \leq \tau \leq 0.1$ . Therefore we simply use such an average for all other nuclei.

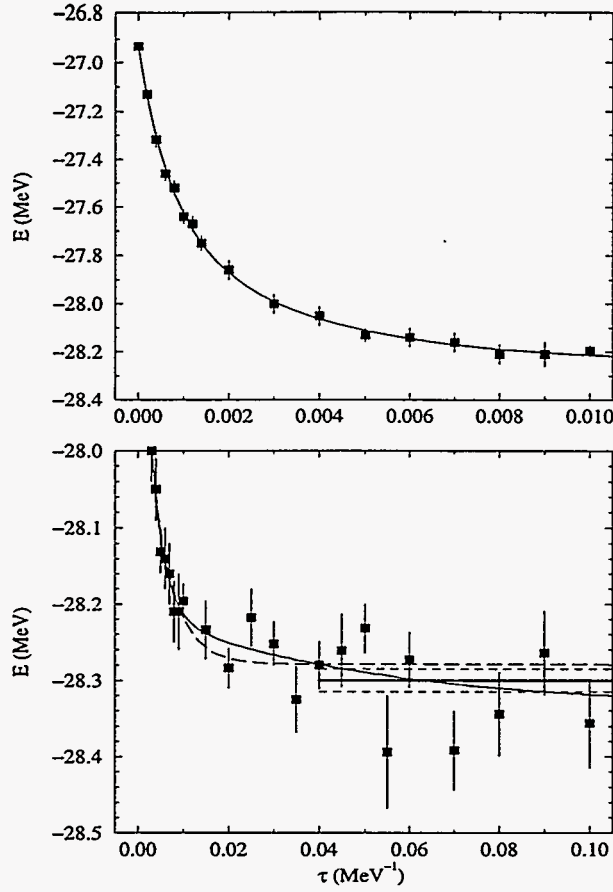


Fig. 1.  ${}^4\text{He}$  GFMC energy as a function of imaginary time. The fits are described in the text.

Because of the difficulties in making useful extrapolations in  $\tau$ , it is important to understand contaminations in  $\Psi_T$ , particularly from low-excitation-energy states which will not be fully filtered out in limited- $\tau$  calculations. We have made several calculations of the ground-state of  ${}^6\text{Li}$  to study the effects of changes in  $\Psi_T$  on the GFMC  $E(\tau)$ . Figure 2 shows the effects of removing some of the noncentral correlations in  $\Psi_T$ ; the solid circles are from a calculation with the full  $\Psi_T$  which includes the NNN correlation based on  $V_{ijk}$ .

The open diamonds were computed by omitting this NNN correlation. This makes the energy at  $\tau = 0$  worse by  $\sim 1.7$  MeV. However by  $\tau = 0.01$ , the GFMC has fully corrected for this defect and thereafter the differences are just statistical fluctuations. Hence removing this NNN correlation enhances the admixtures of excitations  $> 250$  MeV.

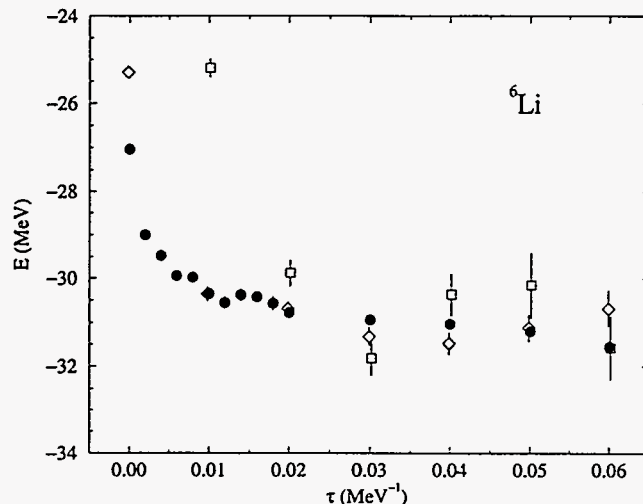


Fig. 2.  ${}^6\text{Li}$  GFMC energy as a function of imaginary time for various truncations of the noncentral parts of  $\Psi_T$ .

The open squares in Fig. 2 come from a much more drastic approximation of  $\Psi_T$ . Here the tensor components of  $F_{ij}$  have also been omitted, resulting in a four-operator wave function. In such a wave function, the dominant tensor components of the two-body potential have zero expectation value and the energy at  $\tau = 0$  is  $+41$  MeV. It is completely corrected by  $\tau = 0.03$ ; again the rate of correction indicates excitation energies  $\sim 250$  MeV. However, the statistical errors from such a bad  $\Psi_T$  are much larger.

These two tests indicate that defects in the non-central parts of the correlation, which have been the subject of much optimization in VMC studies, are easily corrected by the GFMC. Deficiencies in the one-body part of  $\Psi_T$  present more of a problem. The excitation energies corresponding to different  $LS$  components in Eq. 44 are typically 5 to 10 MeV. Thus the  $\beta_{LS}$  must be reliably determined in  $\Psi_T$ .

## 5 Some Results

Table 4. VMC, GFMC, and experimental ground-state (negative numbers) and excitation (positive) energies of  $A = 2 - 8$  nuclei in MeV

${}^A Z(J^\pi; T)$	VMC	GFMC	Expt
${}^2\text{H}(1^+; 0)$	-2.2248(5)		-2.2246
${}^3\text{H}(\frac{1}{2}^+; \frac{1}{2})$	-8.32(1)	-8.47(1)	-8.48
${}^4\text{He}(0^+; 0)$	-27.78(3)	-28.30(2)	-28.30
${}^6\text{He}(0^+; 1)$	-24.87(7)	-27.64(14)	-29.27
${}^6\text{He}(2^+; 1)$	1.86(10)	1.80(18)	1.80
${}^6\text{Li}(1^+; 0)$	-28.09(7)	-31.25(11)	-31.99
${}^6\text{Li}(3^+; 0)$	2.93(10)	2.72(36)	2.19
${}^6\text{Li}(0^+; 1)$	3.84(10)	3.94(23)	3.56
${}^6\text{Li}(2^+; 0)$	4.23(11)	4.43(39)	4.31
${}^6\text{Li}(2^+; 1)$	5.64(10)		5.37
${}^6\text{Li}(1^+; 0)$	5.68(11)		5.65
${}^7\text{He}(\frac{3}{2}^-; \frac{3}{2})$	-20.43(12)	-25.16(16)	-28.82
${}^7\text{Li}(\frac{3}{2}^-; \frac{1}{2})$	-32.78(11)	-37.44(28)	-39.24
${}^7\text{Li}(\frac{1}{2}^-; \frac{1}{2})$	0.33(16)	0.76(41)	0.48
${}^7\text{Li}(\frac{7}{2}^-; \frac{1}{2})$	5.48(16)	5.72(41)	4.63
${}^7\text{Li}(\frac{5}{2}^-; \frac{1}{2})$	6.64(16)	6.56(45)	6.68
${}^8\text{He}(0^+; 2)$	-19.71(18)	-25.77(61)	-31.41
${}^8\text{He}(2^+; 2)$	2.34(25)		2.6
${}^8\text{Li}(2^+; 1)$	-29.70(19)	-38.26(19)	-41.28
${}^8\text{Li}(1^+; 1)$	1.19(26)		0.98
${}^8\text{Li}(3^+; 1)$	2.81(25)		2.26
${}^8\text{Li}(4^+; 1)$	5.63(26)		6.53
${}^8\text{Be}(0^+; 0)$	-48.06(27)	-54.66(64)	-56.50
${}^8\text{Be}(2^+; 0)$	3.90(37)		3.04
${}^8\text{Be}(4^+; 0)$	11.96(35)		11.4

These lectures are primarily about Monte Carlo methods for nuclear physics, so I will present only results for the computed energies of nuclei here. Many other results may be found in [1]. Table 4 shows the ground-state energies and excitation energies of several excited states for nuclei up to  $A = 8$ . Only statistical errors are shown for the Monte Carlo calculations; we believe that the GFMC calculations are converged to  $\sim 0.3$  MeV for  $A = 6$  and  $\sim 0.6$  MeV for  $A = 8$ . The GFMC ground state results show that the Hamiltonian being used underbinds the  $p$ -shell nuclei more and more as  $A$  increases. Also the underbinding becomes worse as one moves away from  $Z = N$ , indicating an isospin problem. A comparison of the VMC and GFMC

results shows that our variational wave functions are much poorer for the  $p$ -shell than for the 3- and 4-body nuclei. However, wherever we have done GFMC calculations for excited states we find that the VMC excitation energies are reliable. Thus the failure of the variational wave function appears to be a bulk property with little state dependence. The computed excitation energies are in quite good agreement with experiment, indicating that failure of the Hamiltonian is also principally a bulk feature.

As is shown in Table 1, there has been much recent progress in nuclear QMC calculations. The present results show that we must make improvements on all fronts: the Hamiltonian, the variational wave function, and GFMC methods for calculations to larger  $\tau$ .

## 6 Acknowledgments

I am indebted to R. B. Wiringa for much help in preparing this paper. This work was supported by the U. S. Department of Energy, Nuclear Physics Division, under contract No. W-31-109-ENG-38. This paper was completed while I was a guest at the Institute for Nuclear Theory at the University of Washington.

## References

1. B. S. Pudliner, V. R. Pandharipande, J. Carlson, S. C. Pieper, and R. B. Wiringa, Phys. Rev. C **56**, to be published (Oct. 1997).
2. J. A. Carlson and R. B. Wiringa, in *Computational Nuclear Physics 1*, edited by K. Langanke, J. A. Maruhn, and S. E. Koonin (Springer Verlag, Berlin, 1991).
3. R. B. Wiringa, V. G. J. Stoks, and R. Schiavilla, Phys. Rev. C **51**, 38 (1995).
4. B. S. Pudliner, V. R. Pandharipande, J. Carlson, and R. B. Wiringa, Phys. Rev. Lett. **74**, 4396 (1995).
5. J. R. Bergervoet, P. C. van Campen, R. A. M. Klomp, J.-L. de Kok, T. A. Rijken, V. G. J. Stoks, and J. J. de Swart, Phys. Rev. C **41**, 1435 (1990).
6. V. G. J. Stoks, R. A. M. Klomp, M. C. M. Rentmeester, and J. J. de Swart, Phys. Rev. C **48**, 792 (1993).
7. J. Fujita and H. Miyazawa, Prog. Theor. Phys. **17**, 360 (1957).
8. S. A. Coon, M. T. Peña, and D. O. Riska, Phys. Rev. C **52**, 2925 (1995).
9. G. E. Brown, W. Weise, G. Baym, and J. Speth, Comments Nucl. Part. Phys. **17**, 39 (1987).
10. J. L. Forest, V. R. Pandharipande, and J. L. Friar, Phys. Rev. C **52**, 568 (1995).
11. J. L. Forest, V. R. Pandharipande, J. Carlson, and R. Schiavilla, Phys. Rev. C **52**, 576 (1995).
12. R. B. Wiringa, Rev. Mod. Phys. **65**, 231 (1993).
13. R. B. Wiringa, Phys. Rev. C **43**, 1585 (1991).
14. S. C. Pieper, R. B. Wiringa, and V. R. Pandharipande, Phys. Rev. C **46**, 1741 (1992).

15. B. S. Pudliner, University of Illinois Thesis (1996).
16. R. Schiavilla, V. R. Pandharipande, and A. Fabrocini, Phys. Rev. C. **40**, 1484 (1989).
17. J. Carlson, Phys. Rev. C **36**, 2026 (1987).
18. J. Carlson, Phys. Rev. C **38**, 1879 (1988).
19. V. R. Pandharipande and R. B. Wiringa, Rev. Mod. Phys. **51**, 821 (1979).
20. D. M. Ceperley, Rev. Mod. Phys. **67**, 279 (1995).
21. K. E. Schmidt and M. A. Lee, Phys. Rev. E **51**, 5495 (1995).
22. M. H. Kalos, J. Comp. Phys. **2**, 257 (1967).
23. D. M. Ceperley and M. H. Kalos, in *Monte Carlo Methods in Statistical Physics*, edited by K. Binder (Springer-Verlag, Heidelberg, 1979).